ELSEVIER

Tectonophysics 248 (1995) 21–37

TECTONOPHYSICS

Computer modelling of granular material microfracturing

D.F. Malan [1], J.A.L. Napier

Division of Mining Technology, CSIR, Johannesburg, South Africa

Received 01 September 1994; accepted 08 February 1995

Abstract

Microscopic observations indicate that intra- and transgranular fracturing are ubiquitous processes in the damage of rock fabrics. Extensive modelling of intergranular fracturing has been carried out previously using the distinct-element approach. The current work is aimed at extending these results to include intra- and transgranular fracturing. Numerical experiments have been carried out to simulate these microfractures in granular media using a boundary-element computer code DIGS. Grains were represented by straight-sided polygons generated with a Voronoi generator. Experiments were carried out to simulate experimental microfracture studies of quartzite in triaxial extension tests. The results support the experimental observations that the microcracks induced by compressive stress are extensile and sub-parallel to the direction of maximum compressive stress. Various mechanisms of microcrack initiation were identified. Some cracks were found to be generated from inside the grains in a manner similar to a Brazilian test. Sliding cracks were found to start from grain boundaries as intergranular cracks and propagate as intragranular wing cracks in the direction of maximum compression. Pores were also modelled as a possible mechanism for microcrack initiation but were found to generate fractures in unexpected directions relative to the direction of applied loading.

1. Introduction

The study of microfracture generation and propagation in rock under compression is essential for understanding basic tensile, extension and shear modes of fracturing and the eventual fracture distribution observed in underground workings. Early investigators have performed a vast number of experiments on crack growth under compressive stress (e.g., McClintock and Walsh, 1962; Brace and Bombolakis, 1963; Hoek and Bieniawski, 1965; Horii and Nemat-Nasser, 1985). Various studies predicted that microcracks generated under compression are extensile in nature (e.g., Brace and Bombolakis, 1963; Hallbauer et al., 1973; Kranz, 1983). These models were confirmed by experimental electron microscopy work (e.g., Tapponier and Brace, 1976; Wong, 1982; Fredrich et al., 1989; Zheng, 1989).

Although a large volume of experimental evidence has become available, a difficulty most researchers have encountered is to explain the interaction and coalescence of the microcracks to form micro-extension fractures or shear bands. The reason is that only global responses of a granular medium can be monitored in experimen-

[1] Present address: Division of Mining Technology, CSIR, P.O. Box 91230, Auckland Park, 2006, South Africa.

SSDI 0040-1951(95)00019-4

tal work while information of the micro-processes is needed. A possible solution is to use numerical simulations of granular media to provide this information. Numerical modelling is more flexible than physical modelling in that any data are accessible at any stage of the test. Naturally, such numerical experiments have to be compared with physical reality when candidate failure mechanisms have been identified. The following noteworthy numerical modelling of micro-processes is described in the literature.

Cundall and Strack (1979) used a distinct-element program BALL to model the behaviour of an assembly of discs. The results gave a very good comparison with an experimental test of an assembly of discs where the photoelastic technique was used. Based on this comparison, the authors concluded that the distinct element method is a valid tool for research into the behaviour of granular assemblies. However, with this program grains are restricted to a circular geometry giving a high void to grain ratio. Splitting of grains is also not possible. Cundall (1989) used the same methodology embodied in TRUBAL to model shear localisation in an assembly of 1000 discs. This gave qualitative agreement with theoretical predictions described in the literature.

Zheng (1989) used a simple numerical model based on the displacement discontinuity principle to model the interaction of extensile microcracks to form shear bands. The model consisted of a statistical distribution of grain centres in an infinite medium. Brazilian-type extensile cracks were generated in virtual grains if a local tension existed in the grain equal to the tensile strength of the grain. In a Brazilian test, a circular disc is compressed in a diametral plane between surfaces that apply concentrated loads. Increasing the load will result in a tensile fracture forming along the loaded diameter (see e.g., Malan et al., 1994). In Zheng's model, this process of Brazilian crack formation was continued until failed grains formed an en échelon shear band pattern across the specimen. Grain boundaries, however, were not explicitly modelled and therefore the various mechanisms generating microcracks could not be investigated. The model also did not allow for the formation of intergranular fracturing (fracturing occurring on the boundaries between grains). Explanations of the establishment of en échelon patterns have been given by Du and Aydin (1991) and Olson and Pollard (1991). Horii and Nemat-Nasser (1985) have carried out extensive theoretical analysis and have performed physical experiments with perspex plates to demonstrate mechanisms for the coalescence into shear bands of extension fractures initiated at the ends of randomly located sliding cracks.

Kemeny and Cook (1987) used micromechanical models for splitting and shear faulting to investigate parameters associated with rock fracture under compressive stresses. The axial splitting model consisted of a two-dimensional body containing a column of sliding cracks and the shear zone model consisted of a collinear row of cracks. They have demonstrated overall material response to loading depending on an analysis of the stress intensity factors associated with these crack assemblies. No detailed simulation of crack growth was, however, carried out.

Kemeny and Cook (1991) reviewed the fracture mechanical representation of a cylindrical pore model, a sliding crack model, an elastic mismatch model, a dislocation pile-up model and a hertzian crack model as possible models for crack growth under compression. Because of the similarity of these mechanisms, a generic model was proposed to take into account all of the above phenomena. It was shown how these micromechanical models can form the basis for continuum damage models using the finite element method. Numerical analysis of a thick-walled cylinder predicted an elliptically shaped breakout region similar to experimental results.

Reches and Lockner (1994) presented a model for the nucleation and growth of faults in brittle rocks. It was suggested that initial tensile microcracking occurs randomly with no significant crack interaction. As the load increases, the tensile microcracks interact to produce a process zone. As the process zone lengthens, its central part yields to form a fault nucleus. The stress fields associated with the overall shearing enhance microcrack dilation in the process zone. This allows for the propagation of both the process and shear zones. The model predicted that a shear zone

should propagate in its own plane making an angle of 20–30° with the axis of maximum compression which is in agreement with the bulk of experimentally formed shear zones. The formation of the central nucleus from the initial microcracking is, however, not explicitly modelled.

Innovative modelling of granular media has been carried out by Handley (1993) using the program UDEC (Cundall and Hart, 1983). The granular medium is modelled as an assembly of distinct elements that can interact with each other according to the fundamental laws of Newtonian mechanics. The results of simulated uniaxial loading tests compared very well with laboratory findings with the exception that load was regenerated following the initial stress drop after the peak load. No through-grain fracturing was allowed in this model. However, experimental evidence presented here indicates that intragranular (through-grain fracturing not propagating across grain boundaries) and transgranular (intragranular fracturing propagating across grain boundaries) fracturing are ubiquitous processes in the damage of rock fabrics. The aim of the work described in this paper is therefore to extend the above-mentioned work by addressing the following three questions:

(1) Can the initial intra- and transgranular fracture growth in a granular medium be modelled by using a small-strain approach to simulate fractures and grain boundaries as distributed dislocations?

(2) Can mechanisms for the generation of tensile fractures in a compressive stress field be identified and modelled?

(3) Will it be possible to model the coalescence of the microfractures to form a shear band?

2. The Voronoi generator

Following Handley (1993), a Voronoi polygon generator was used to generate random assemblies of grains. A Voronoi polygon structure comprises randomly generated polygons that cover a spatial region with no gaps between adjacent polygons. This structure is generated using an algorithm that allows the spatial region to be partitioned around a random set of geometric centres in such a way that each polygon represents the region closer to a given centre than any other centre. As the structure consists of flat-sided polyhedra perfectly packed together, there is an interdependence in the shape between any polygon and its neighbours (Brostow et al., 1978; Finney, 1979).

The Voronoi polygon associated with a given centre, i, in an assembly of N centres is defined as that area of space containing all points closer to i than to any other centre j. Although not a true representation of all types of rock (voids between grains are absent), such a generator provides a reasonable approximation of the underlying granular structure and allows any number of geometries to be generated quickly. The procedure used for generating the polygons is described by Finney (1979). In contrast to the approach of Brostow et al. (1978), this method first calculates potential vertices and then joins the selected vertices. The distribution of the geometric centres determines the granular geometry. When using different initial distributions of geometric centres, different granular geometries can be generated (the geometries are different but the average grain size and mean deviation from average size are the same). For the purpose of this study the Voronoi generator was modified to include a grain parameter k to modify the size distribution of the grains. This parameter is used as follows:

$$R_{\min} = \frac{kL}{(N)^{1/2}} \qquad 0 < k < 1 \qquad (1)$$

where $R_{\min}$ is the minimum distance between any centre i and centre j ($i \neq j$), L is the side-length of a square boundary and N is the number of geometric centres.

A new centre generated by the random generator is only accepted if it is not closer than $R_{\min}$ to any of the existing centres. This process is continued until N centres are generated. It is clear from this that as k becomes closer to unity, more candidate centres will be rejected. This is illustrated in Fig. 1a. The effect of k on the average grain size and deviation from average

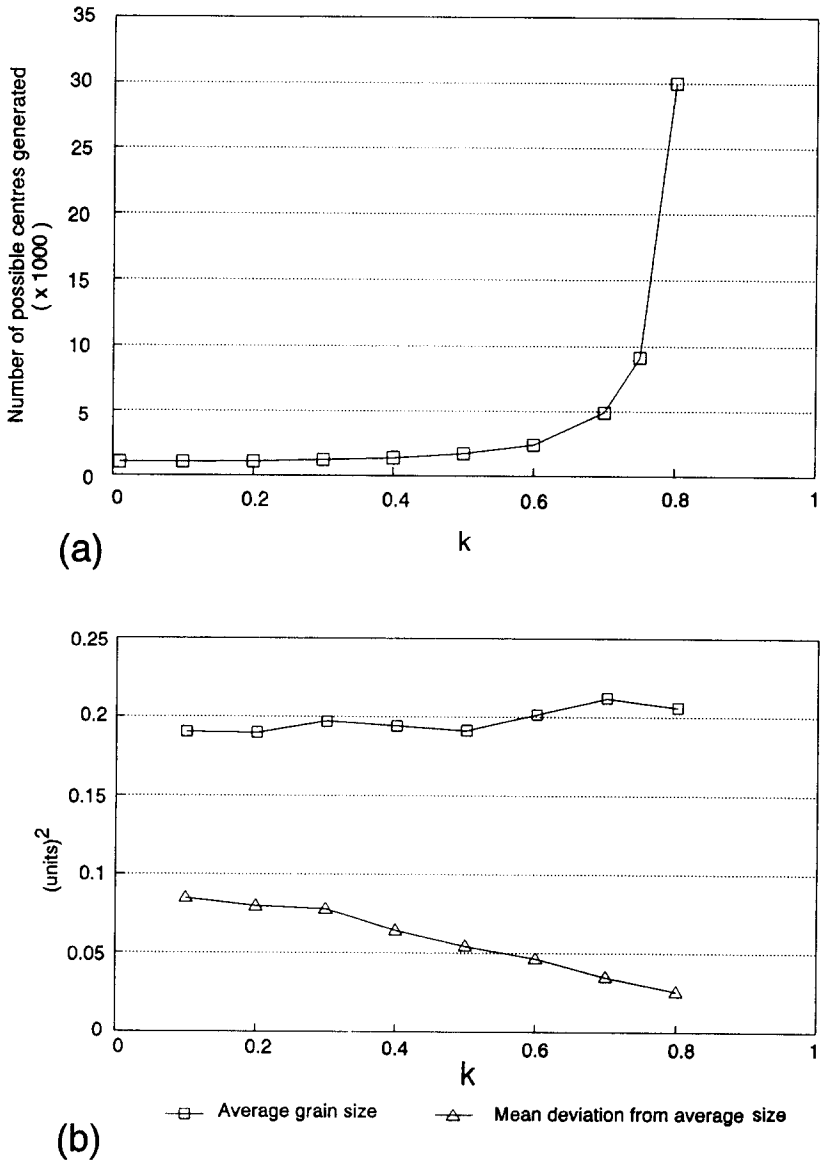

Fig. 1. (a) The number of possible centres generated as a function of the grain parameter k to generate a 1000 true centres. (b) The effect of the parameter k on the average grain size and mean deviation from average size.

Table 1
Grain statistics

	k	Number of grains	Average grain size (arb. units^2)	Mean deviation from grain size (arb. units^2)
Sample 1	0.8	72	0.5555	0.0641
Sample 2	0.5	82	0.5092	0.1162
Sample 3	0.3	82	0.5024	0.1527

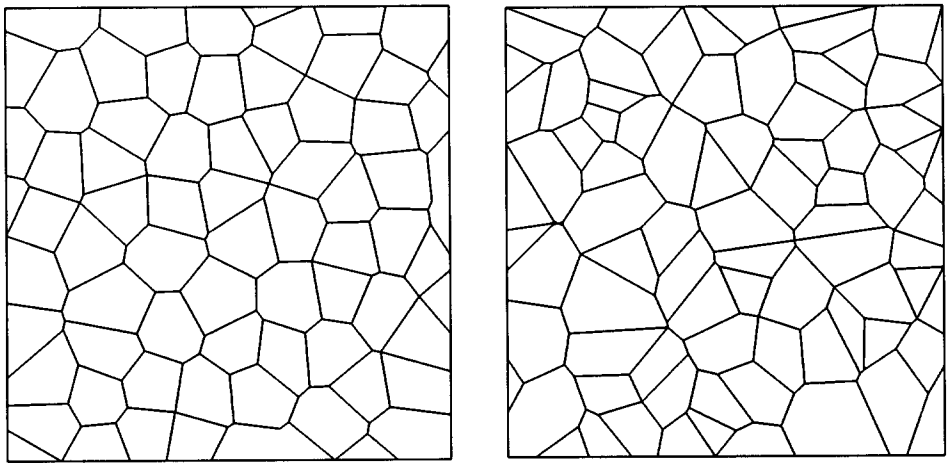

Fig. 2. Grain geometries generated with the Voronoi generator to show the effect of the grain parameter k.

size is shown in Fig. 1b. As k becomes bigger, the size of individual grains becomes more uniform. Typical geometries generated by selecting values of $k = 0.3$ and 0.8 are displayed in Fig. 2. Three geometries with values of $k = 0.3$, 0.5 and 0.8 were used to model the triaxial extension test described later. The grain statistics for these geometries are displayed in Table 1.

3. Simulation of fracture growth

A displacement discontinuity program DIGS (Discontinuity Interaction and Growth Simulation) was used to model failure in the granular geometries. The technique for fracture growth used in this paper is based on previous studies of fracture growth near openings in highly stressed brittle material (Napier, 1990; Napier and Hildyard, 1992; Napier and Ozbay, 1993). A more complete description of the program can also be found in Malan et al. (1994). Fractures and boundaries between grains were represented by linearly varying displacement discontinuity elements joined end to end. The current version of the program is limited to 500 elements on a microcomputer equipped with 32 Mbytes of memory.

Evidence in the literature indicates that induced microcracks in rock are extensile in nature, even in a compressive loading environment. Fractures within grains were therefore modelled as tensile fractures. Fracture growth is controlled by evaluating the stress field at a set of potential nucleation sites or "seed points". Although these potential growth sites are reminiscent of flaws as interpreted in a Griffith model, the seed points are not explicitly modelled as Griffith cracks but are assumed to propagate when the local stress reaches the specified failure surface. The seeds for this granular study are located at the junction of grain boundaries but only one seed is specified within each grain. In principle, multiple seeds could be introduced in each grain, but this has not been explored in the paper.

For tensile fracture growth from the seed points, the measure of the propensity for crack growth is deemed to be the magnitude of the most tensile principal stress component evaluated at the centroid. If the orientation of this component is at an angle α with respect to a specified global coordinate system, then it is assumed that

the fracture will grow in either the direction $\alpha_1 = \alpha + \pi/2$ or $\alpha_2 = \alpha - \pi/2$. To make the choice specific, a base angle β is associated with each seed point and the angle α_i, where $i = 1, 2$, that is closest to β is chosen as the growth direction. In the case of a growing fracture, the base angle, β, is assumed to be the angle of the last element in the segment and the optimum growth angle is found by a direct search of the stress field at points on the circumference of a circle of radius ρ, centred on the crack tip. In the case of extension fracture growth, the optimum growth direction is assumed to be the radius connecting the crack tip to the circumferential position, P, where the angular stress component $\tau_{\theta\theta}$, parallel to the circumference, is a maximum (assuming tensile stresses are positive). The direct search method is used because it is more robust in avoiding oscillations in the crack growth path that can occur if the growth direction procedure is based on local estimates of the crack tip stress intensity factor (Thomas and Pollard, 1993).

In the present series of numerical experiments, a single crack increment is chosen from all the available growth sites by selecting the overall maximum value of $\tau_{\theta\theta}$ determined at each site. A single element is then introduced at the optimum site in the appropriate direction and the entire problem is resolved with the additional element. The search procedure is then repeated using the new problem solution. This process ceases when it is found that the element that would be introduced at the optimum site, would not be mobilised, according to a specified failure criterion, evaluated at the chosen seed point or position P ahead of the crack tip. The failure criterion is assumed to be given by a bilinear relationship defined by the bounds:

$$\sigma_1 = -\sigma_c + m\sigma_3 \quad (2)$$

$$\sigma_3 = T_C \quad (3)$$

where σ_c = uniaxial compressive strength, σ_3 = minor principal stress component, σ_1 = major principal stress component (note $\sigma_1 < \sigma_3$ for a negative compressive stress convention), m = slope of the failure surface and T_C = maximum tensile strength of the material.

4. Microfracture modelling of quartzite in triaxial extension

As a practical example, numerical modelling of triaxial extension tests in quartzite was conducted to compare the simulated fracture growth with microfractures observed in actual tests. These experimental tests were conducted to simulate the stress environments around stopes in deep-level goldmines (Briggs and Vieler, 1984). In these experiments the intermediate (σ_2) and maximum (σ_1) principal stresses were equal and applied radially to the rock sample (covered by a rubber sleeve) by a confining fluid. The minimum principal stress (σ_3) was applied axially by the platens of the testing machine. Initially the sample was loaded hydrostatically to the desired confinement and then the axial stress (σ_3) was reduced until the specimen failed.

The quartzite used is a siliceous quartzite from the Millar reef in the MB5 zone in the Vaal Reef Basin near Klerksdorp in South Africa and of Precambrian age. The material for testing was obtained by drilling holes parallel to bedding in the underground workings. Suitable sections of core were machined to produce cylinders of 76.2 mm length and 25.4 mm diameter. The quartz content of the samples varied from 89 to 94% of which 87–93% comprised quartz grains. The remainder occurred as fine interstitial material. Other minerals in the rock were sericite, chert, pyrite and mica. The average grain size was about 0.5 mm. Experimental values of Young's modulus and the failure parameters defined in Eq. (2) were $E = 70$ GPa, $\sigma_c = 320$ Mpa and $m = 9.32$, respectively.

A typical example of a stress–strain curve for the extension test is shown in Fig. 3. Elastic strain is defined by extending the linear portion of the curve to a point where it intersects the line parallel to the strain axis dropped from the failure point. Plastic strain is the strain difference between the point of intersection and the failure strain. The specimen was loaded along a hydrostatic path by increasing the pressure of the confining fluid (σ_1 and σ_2) and the axial loading (σ_3) at the same rate. When the desired hydrostatic pressure had been attained, the axial force was

gradually relaxed until a predefined degree of extension had been achieved or until the sample failed. If the test was stopped at a predefined degree of extension, the axial load was reapplied to achieve hydrostatic loading before unloading the specimen. The laboratory tests were stopped at various degrees of extension to characterise the microscopic behaviour of the quartzite in the pre-failure region. After removal the specimens were impregnated with resin, cut in half axially and polished. When viewed under reflected light microscopy, microfractures were clearly visible.

At a level of 42% of the expected axial strain to failure (before plastic strain has occurred) intragranular cracks parallel to the maximum principal stress were observed (Fig. 4a). The intensity of the intragranular fractures increased with further extension. At 75% of the expected axial strain to failure, transgranular fracturing became visible as shown in Fig. 4b. Note that several parallel fractures can occur in the same grain. Very few grain-to-grain contacts were broken indicating that intergranular fracturing is minimal in this rock type. With further extension, intra- and transgranular fracturing became intense in certain areas of the specimen. Eventually, coalescence of these fractures led to the formation of a shear zone and failure of the sample (Fig. 4c). The angle of the failure plane for this sample was 78° with respect to the σ_3-direction marked by an arrow in Fig. 4c. The density of the fractures increased towards the failure surface from both directions. The average fracture density (fractures/mm) as a function of axial strain is displayed in Fig. 5. The density was calculated by traversing a microscope along the centreline of the axis of each specimen for a distance of 2 mm. The different fractures were counted and divided by the length of the traverse. The density of intragranular fracturing increases almost exponentially with strain. The density of transgranular fracturing is much lower and only starts at a higher level of strain.

To model this triaxial extension test in two dimensions, three geometries with values of k = 0.3, 0.5 and 0.8 were used. As mentioned previously, the simulations are limited to 500 elements (growth elements included). Therefore the size of

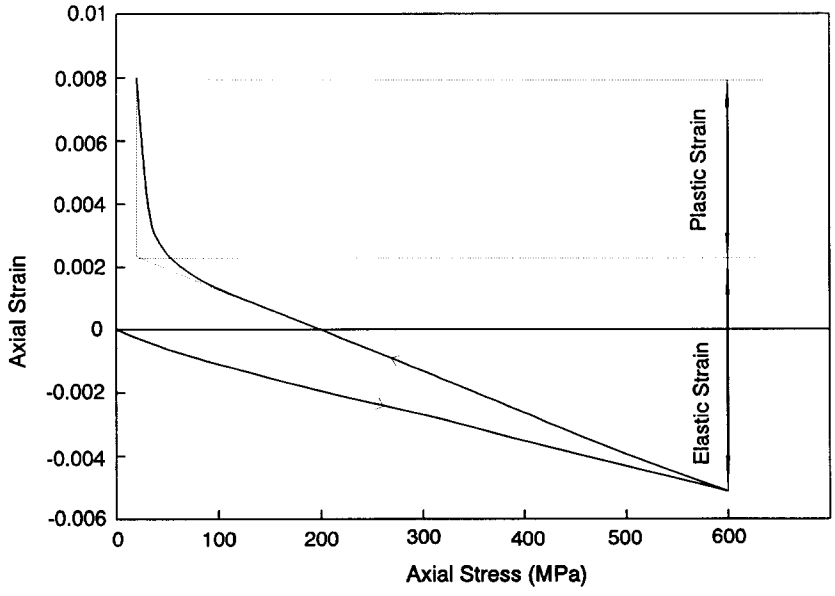

Fig. 3. Typical example of the stress–strain curve for a triaxial extension test on quartzite. This shows the decomposition of the strain into elastic and plastic components.

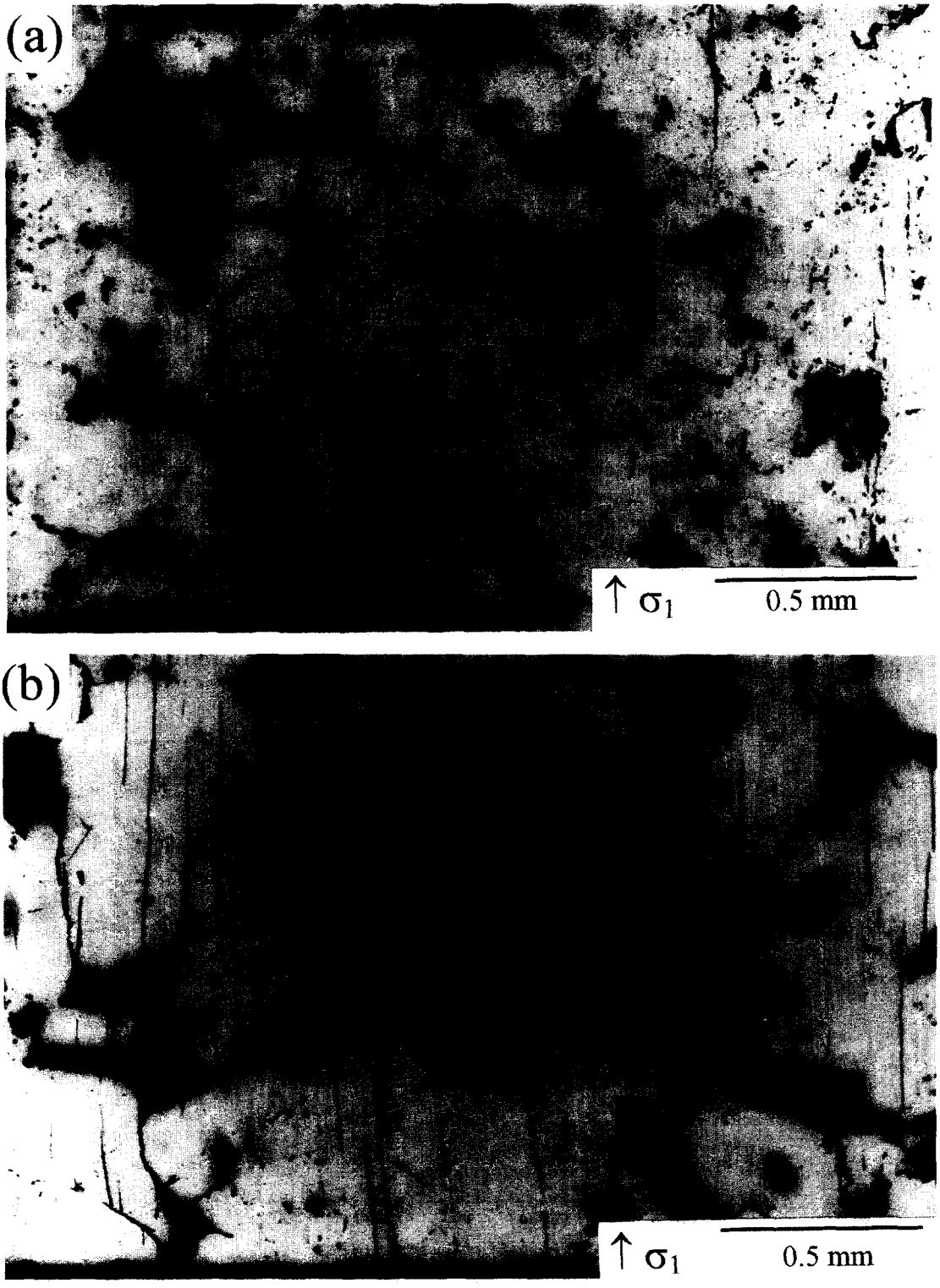

Fig. 4. (a) Initial intragranular fracturing in quartzite. (b) Intragranular fractures propagate across grain boundaries to form transgranular fractures. (c) Coalescence of microfractures to form a failure surface.

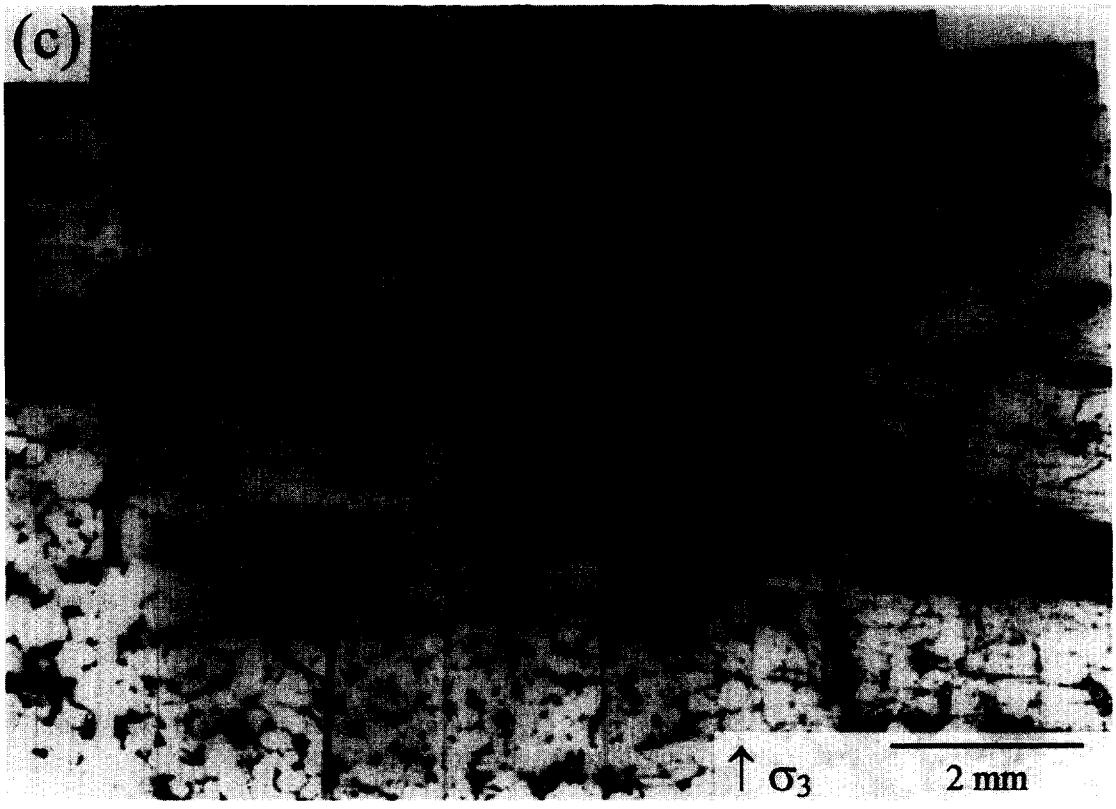

Fig. 4 (continued).

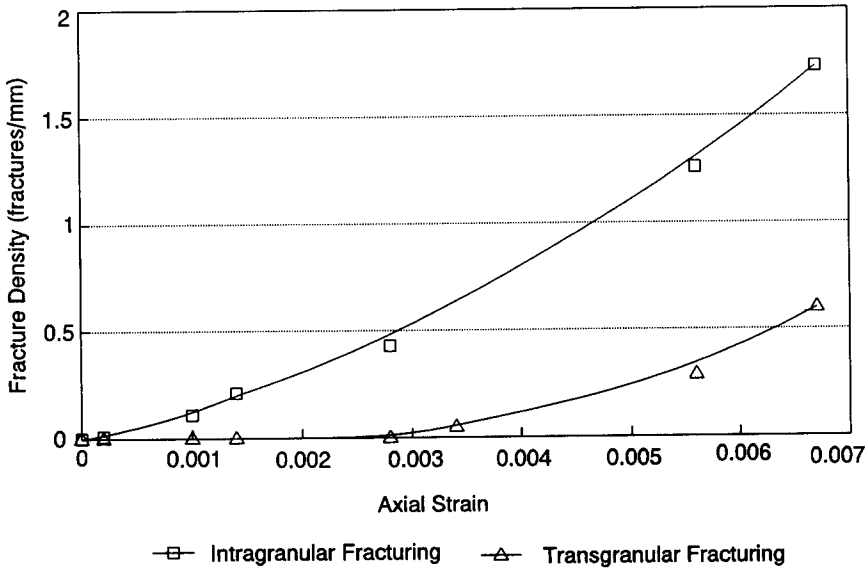

Fig. 5. Experimental fracture density as a function of strain.

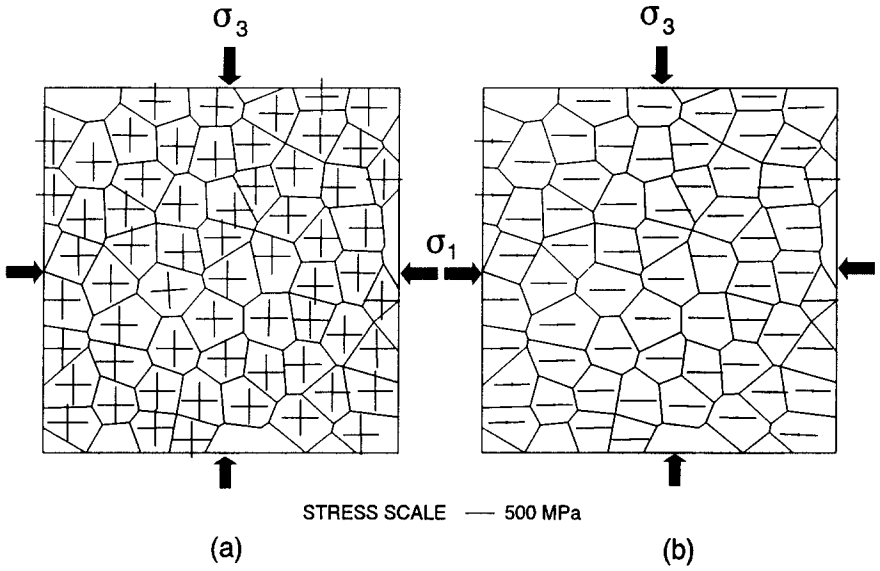

Fig. 6. Principal stresses in the numerical test (Sample 1) showing (a) the initial hydrostatic loading conditions and (b) the stresses before the onset of fracturing.

each sample was limited to about 80 grains (Table 1) to allow appreciable fracture growth to take place. The interfaces between the grains were given properties similar to the experimental rock strength properties corresponding to the overall sample strength. Traction boundary conditions were applied to load the samples to a hydrostatic stress state of 600 MPa. The principal stresses in Sample 1 for this condition are displayed in Fig. 6a. The axial traction (vertical axis) was then reduced incrementally to initiate fracture growth. The principal stresses just before fracturing commenced are shown in Fig. 6b. Fractures initiated at an axial strain of 0.0014. The final fracture pattern for Sample 1 is shown in Fig. 7. The similarity with the experimental samples in Fig. 4b is immediately evident. There is a high density of intragranular fracturing with several transgranular fractures visible. The fractures are sub-parallel to the maximum principal stress and in some areas several parallel fractures can occur in the same grain. The geometry in Fig. 7 is distorted (displacements ten times enlarged) to illustrate where grain-to-grain contacts (intergranular fracturing) were broken. The density of this is low, compared to intra- and transgranular fracturing. Similar behaviour was noted in the experimental tests.

When modelling granular assemblies, it is important to include the effect of intra- and transgranular fracturing. To prove this statement the simulations were repeated without allowing

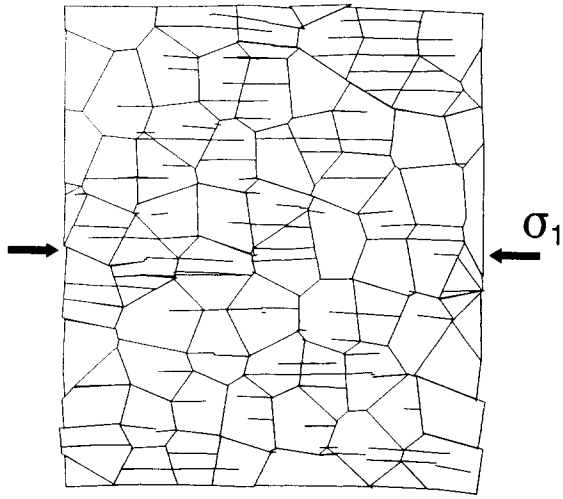

Fig. 7. Intra-and transgranular fracturing in Sample 1. The grain displacements are exaggerated (10× enlarged) to indicate where grain-to-grain contacts were broken.

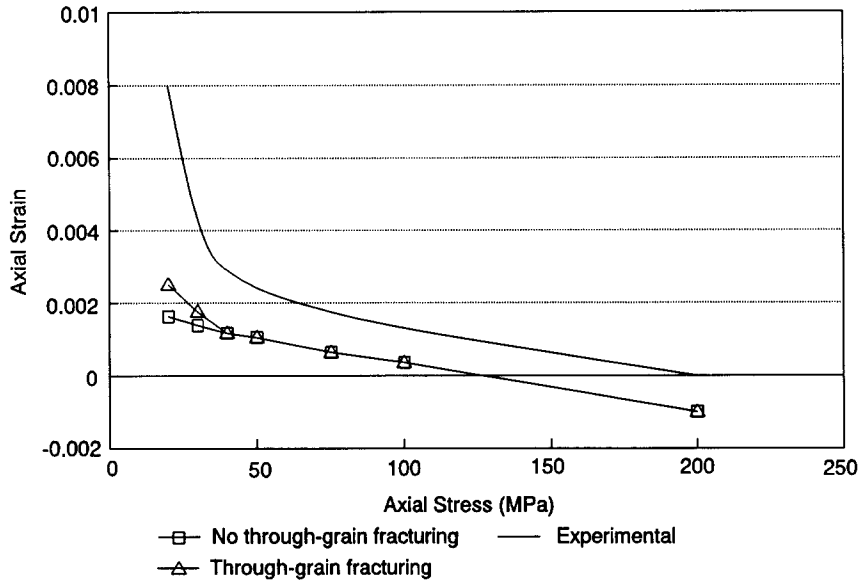

Fig. 8. Numerical stress–strain curves indicating the effect of grain fracturing.

through-grain fractures to initiate. The stress–strain curves for Sample 2 with and without through-grain fracturing are displayed in Fig. 8 to illustrate the typical behaviour (the full curve is not displayed). The experimental curve is displayed for comparison purposes. It is clear that by doing the simulation with through-grain fracturing leads to an increase in axial strain at low stresses and thus approaches the experimental curve more closely.

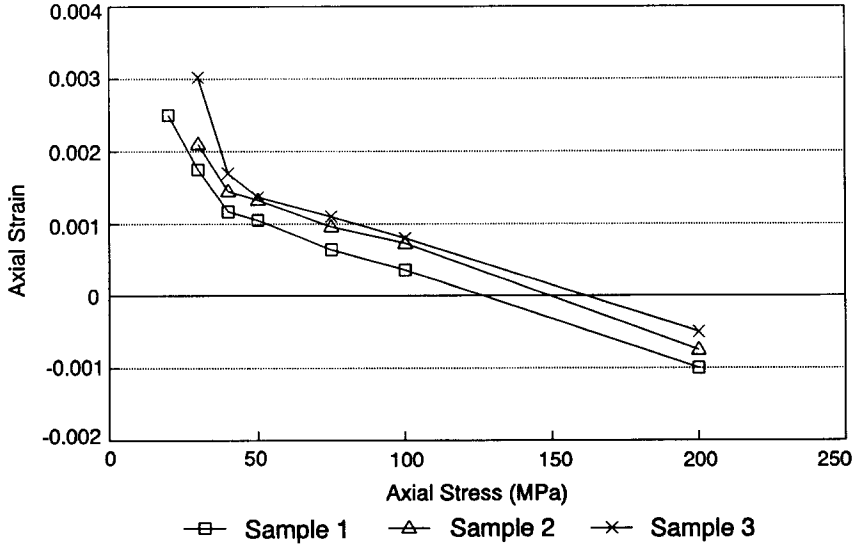

Fig. 9. The effect of grain geometry on the stress–strain curve.

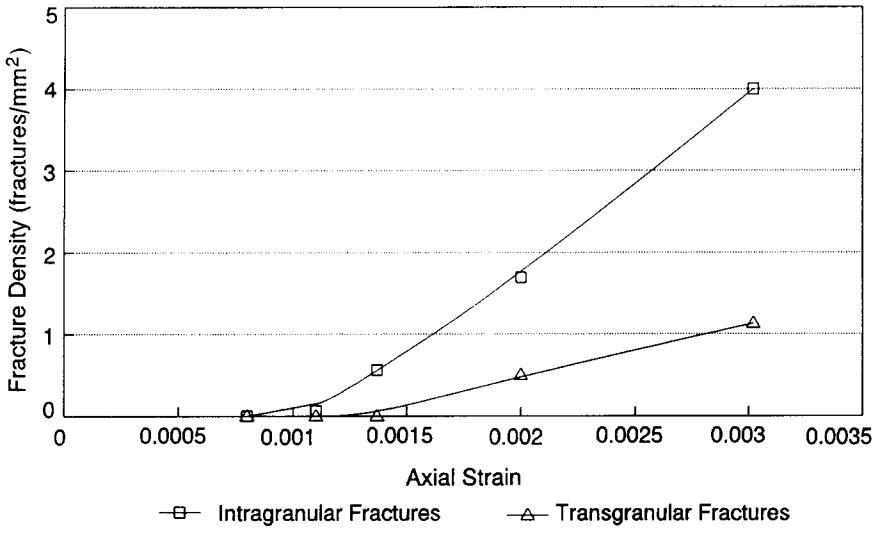

Fig. 10. Simulated fracture density as a function of strain.

The stress–strain curve for samples 1, 2 and 3 with through-grain fracturing are compared in Fig. 9 to illustrate the effect of grain geometry (all other parameters were identical). The curves are parallel with the increased axial strain effect clearly evident. It is apparent that for the more rounded and equal-sized grains (Sample 1), the material is stronger with less deformation for the same axial stress. This difference is caused by the geometry of the grains which allow more slip to take place in Sample 3 compared to Sample 1 where the rounded grains are interlocked. Through-grain fracturing, however, leads to an increase in axial strain at low stresses in all three samples.

The numerical density of intra- and transgranular fracturing as a function of strain is illustrated in Fig. 10. The density of fractures (fractures/mm^2) was calculated by assuming an average grain size of 0.5 mm. Although this be-

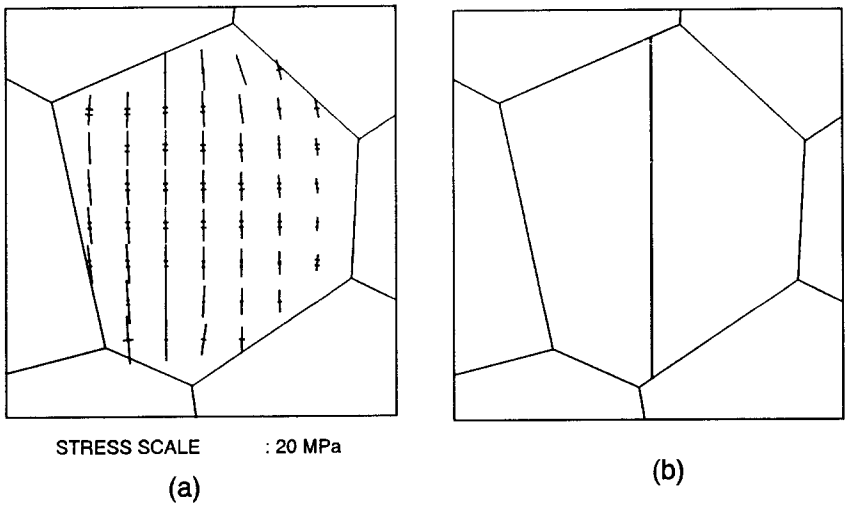

Fig. 11. (a) Principal stresses in a diametrically loaded grain (a double line denotes tension). (b) Axial splitting of the grain.

haviour can not be directly compared to Fig. 5 due to different units and scale, a similar trend is observed with a much bigger increase in intra- than transgranular fracturing density with increasing strain.

5. Mechanisms of microfracture initiation

Various mechanisms of tensile fracture initiation in a compressive field can be identified in the literature namely beam bending, point loading, diametral compression of grains, pores, sliding cracks and hard inclusions (e.g., Gallagher et al., 1974; Olsson, 1974; Lajtai, 1974). Due to the geometry of the Voronoi polygons, no beam bending or point loading were observed in the numerical simulations. Currently DIGS can model only one material type so the effect of hard inclusions was not examined. The remaining micro failure mechanisms were identified and are described below.

In the numerical simulation, some cracks were found to have been generated when diametral compression of grains occurred. These fractures were formed at seed points inside the grains in a manner similar to a Brazilian test and were confined to single grains [see Malan et al. (1994) for an explanation of the Brazilian test]. This mechanism must, however, be seen in perspective. Experimental evidence (Gallagher et al., 1974) indicates that the largest stress concentrations develop near point contacts of grains. Therefore, most microcracks initiate in the vicinity of grain boundaries. This is reproduced in the modelling where in Fig. 7 70% of the fractures initiated at the grain boundaries. Pure Brazilian-like fracturing only occurred in grains where the local stress is such that a high diametral load is imposed with low confinement perpendicular to the local diametral loading direction. This mechanism was prominent in numerical simulations of a uniaxial compressive test (not reported in this paper) where no confinement perpendicular to the loading direction was applied to the sample boundary. In the numerical triaxial extension tests (e.g., Fig. 7), where some confinement was still applied when fracturing initiated, it was not the dominant mechanism of microfracturing. In the actual tests of natural quartzites it also seemed as if the majority of the fractures initiate from the grain edges. There were, however, some fractures observed with both crack tips terminated within the centre region of the grain. This evidence suggests that some fractures can indeed initiate from the centre of grains with possible mechanisms of Brazilian behaviour, flaws or micropores.

The principal stresses in a grain loaded in this manner are shown in Fig. 11a. Note the tension generated (double lines denote tension). These stresses are very similar to the analytical principal stresses calculated for a Brazilian test (Malan et al., 1994). The numerical fracture growth splitting the grain in two is shown in Fig. 11b. This mechanism was first described by Gallagher et al. (1974).

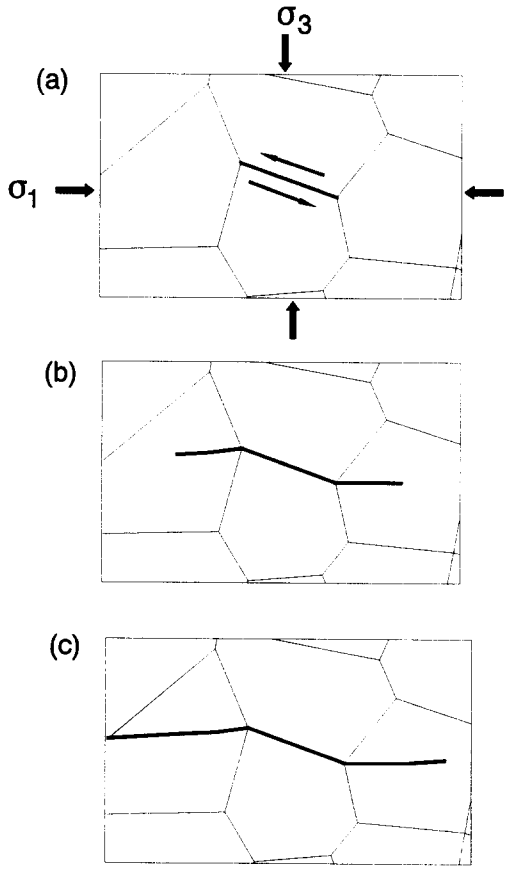

Fig. 12. Sliding cracks as a mechanism of generating extensile intragranular fracturing.

Such cracks were also observed by Olsson (1974) in his experiments on Crown point limestone and by Zheng (1989) using Indiana limestone.

Sliding cracks have been a commonly used model for the generation of tensile fracture growth in a compressive stress field (Hoek and Bieniawski, 1965; Lajtai, 1974; Nemat-Nasser and Horii, 1982; Horii and Nemat-Nasser, 1985; Petit and Barquins, 1988). Zheng (1989) found in granular media that these cracks usually start from grain boundaries as intergranular cracks and then propagate in the direction of maximum compression. In the DIGS models this was a prominent mechanism as is shown in Fig. 12. Slip occurred along an inclined grain contact (thus an intergranular fracture) causing a local tensile zone. This is depicted in Fig. 13 showing the tensile zone at the bottom of a typical sliding interface. The resulting tensile fractures propagated in the direction of maximum principal stress. Nemat-Nasser and Horii (1982) and Ashby and Hallam (1986) derived fracture mechanics models describing the initiation and propagation of wing cracks from a pre-existing inclined fracture in a stress field. According to this theory a critical stress is required to initiate crack growth. The cracks grow until the stress intensity K_I falls below the fracture toughness K_{IC}. Thereafter the cracks grow in a stable way, requiring an increase in stress for each increment of crack growth (if σ_3 is compressive). A similar behaviour was noted for the DIGS sliding cracks. The initial fractures in Fig. 12b formed only after the stress ratio ($\lambda = \sigma_3/\sigma_1$) was equal to 0.048. It remained stable until λ was decreased to 0.017 resulting in extension of the fractures as in Fig. 12c. It was observed in some cases that the two wing cracks for a particular slider did not initiate simultaneously at the same stress ratio. This was a result of different local stress conditions caused by the random distribution of grains throughout the assembly. This emphasises the fact that in a granular assembly a uniformly applied stress is not manifested on a local grain scale.

In previous experimental work many cracks were observed to be generated from pores. This mechanism was suggested by Lajtai (1974), Olsson (1974), Wong (1982) and Zheng (1989). Sammis and Ashby (1986) studied crack growth from a circular hole by loading plates of glass in com-

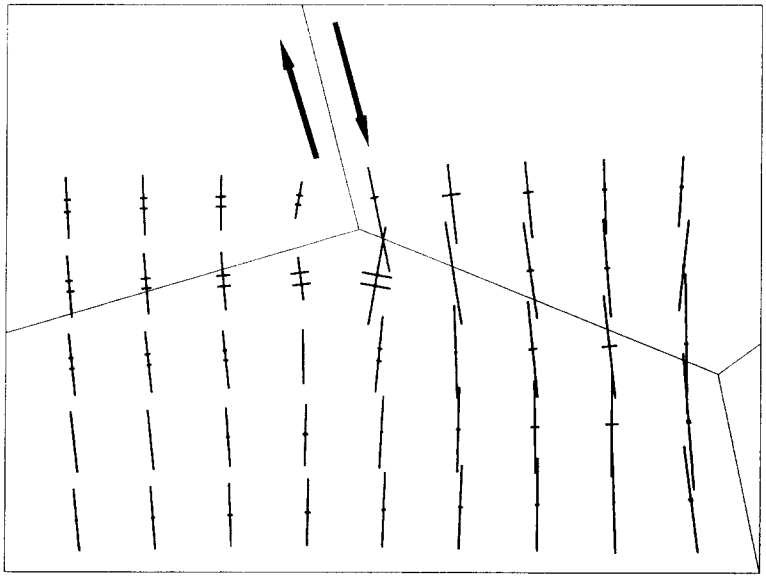

Fig. 13. Principal stresses below a typical sliding crack indicating a local tensile zone (a double line denotes tension).

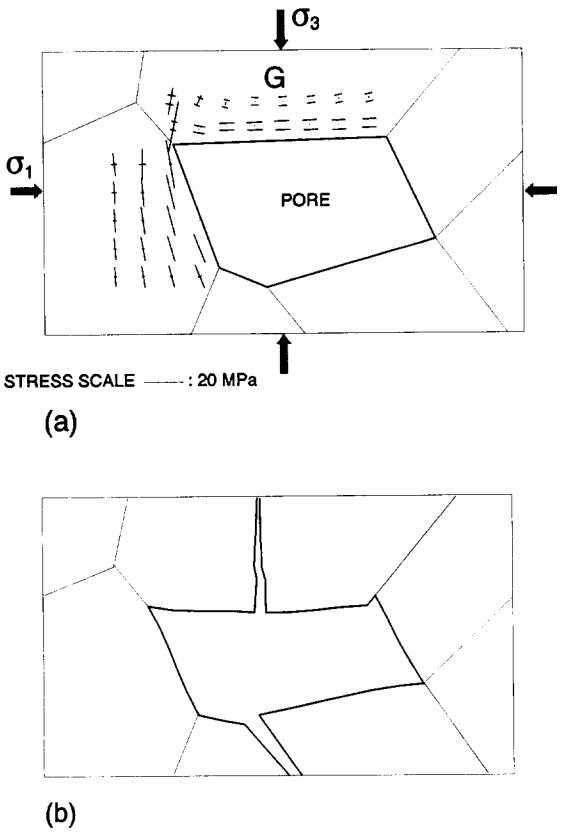

Fig. 14. Numerical simulation of a pore in a granular assembly showing (a) local tensile stresses due to distortion (a double line denotes tension) and (b) the resulting extensile fracture growth.

pression. For a hole subjected to principal stresses σ_1 and σ_3 with $\lambda < 1/3$ the stresses at the top and bottom of the hole (aligned with σ_1) are tensile. This can lead to extensile fractures growing in the direction of maximum principal stress from the edge of the hole. Such a hole is an idealized case whereas pores found in rocks are not perfectly rounded. In order to model pores in the DIGS simulations, the boundaries of several non-adjacent grains were represented as free surfaces. Fig. 14a shows the principal stresses surrounding a typical pore for a stress ratio equal to 0.83. The cause of the tensile stress pattern parallel to the pore boundary is that grain G in Fig. 14a has been distorted. No tensile stresses exist at the sides of the pore aligned with the σ_1-direction for this value of λ. This stress pattern resulted in a fracture growing in the σ_3-direction (Fig. 14b). Fig. 14b has been plotted by magnifying the displaced positions of the grain surfaces to reveal the deformed shape of the pore. In the numerical simulations that were performed, no cases were found in which fracturing was initiated parallel to σ_1 as would be predicted for an idealized model of a circular hole. This implies that care should be taken when applying the pore model to practical samples. It is, however, still important to note that pores modify the local stress field creating local tensile stresses and allowing extensile fractures to form although the fractures caused by this mechanism are not necessarily parallel to the global maximum stress direction. The dominant mechanism of fracturing from pores in the numerical simulations was bending of grains which, for the pores studied, always caused fractures to align with the σ_3-direction. Gallagher et al. (1974) also observed from their experiments, using imitation grains, that bending of grains could result in practically any fracture orientation. However, in the quartzite test samples the bending mechanism could not play a significant role because the porosity was very low and all of the fractures observed were subparallel to the maximum principal stress.

6. Conclusion

The initial through-grain fracturing in quartzite extension tests has been successfully modelled using a displacement discontinuity approach. The fractures are extensile and sub-parallel to the maximum principal stress. In quartzite, the initial microfracturing is mainly intragranular fracturing with transgranular fracturing observed at higher levels of strain. These phenomena were successfully modelled using a displacement discontinuity formulation to represent both grain boundaries and microfractures. In particular, the small strain discontinuity approach is capable of modelling both fractures and individual grain movements including micro-rotations and translations.

A fundamental mechanism for the generation of the fractures under compressive stress is the formation of local tensile stresses. Three differ-

ent mechanisms for the generation of these tensile stresses were identified in the models. Firstly, diametral loading of grains generates tensile stresses along a line which connects the loading points. Secondly, sliding along grain boundaries introduces tensile stresses in adjacent grains which can initiate tensile fracturing parallel to the loading direction. Thirdly, tensile fractures were noted to arise at the boundaries of open pores when the loading ratio σ_3/σ_1 was high (0.83). However, these fractures formed in an unexpected orientation parallel to the σ_3 loading direction and were caused by a bending distortion of the grain surface adjacent to the pore.

No coalescence of the numerical fractures was observed due to the small number of grains used. Memory sizes and computer time limit the current version of DIGS to 500 elements. With the assumption of 0.5 mm grain sizes, the current model can simulate a two-dimensional specimen size of only 25 mm^2. Work is currently being directed to utilise specialised lumping techniques to increase the number of elements to more than a thousand and beyond. This will allow for more grains and possible coalescence of microfractures to be modelled.

Acknowledgements

This work forms part of the Rockmass Behaviour research programme of Rock Engineering, CSIR Division of Mining Technology. The authors wish to acknowledge the financial assistance and support received from the Safety in Mines Research Advisory Committee (SIMRAC). The authors would also like to thank Mr. M.F. Handley for his permission to refer to results from his Ph.D. thesis which is not yet submitted and Dr N.C. Gay and Dr R.G. Gürtunca for several useful comments. Suggestions made by three reviewers contributed significantly to the paper.

References

Ashby, M.F. and Hallam, S.D., 1986. The failure of brittle solids containing cracks under compressive stress states. Acta Metall., 34: 497–510.

Brace, W.F. and Bombolakis, E.G., 1963. A note on brittle crack growth in compression. J. Geophys. Res., 68: 3709–3713.

Briggs, D.J. and Vieler, J.D.S., 1984. Microfracture studies of quartzite in triaxial extension. COMRO (now Miningtek, CSIR, South Africa) Int. Res. Rep. 12/84 1984.

Brostow, W., Dussault, J. and Fox, B.L., 1978. Construction of Voronoi Polyhedra. J. Comp. Phys., 32: 81–92.

Cundall, P.A., 1989. Numerical experiments on localization in frictional materials. Ing.-Arch., 59: 148–159.

Cundall, P.A. and Hart, R.D., 1983. Development of generalized 2-D and 3-D distinct element programs for modelling jointed rock. Final Tech. Rep., U.S. Army Eng. Waterways Exp. Stn.

Cundall, P.A. and Strack, O.D.L., 1979. A discrete numerical model for granular assemblies. Geotechnique, 29: 47–65.

Du, Y. and Aydin, A., 1991. Interaction of multiple cracks and formation of echelon crack arrays. Int. J. Numer. Anal. Methods Geomech., 15: 205–218.

Finney, J.L., 1979. A procedure for the construction of Voronoi polyhedra. J. Comput. Phys., 32: 137–143.

Fredrich, J.T., Evans, B. and Wong, T.-f., 1989. Micromechanics of the brittle to plastic transition in Carrara marble. J. Geophys. Res., 94: 4129–4145.

Gallagher, J.J., Friedman, M., Handin, J. and Sowers, G.M., 1974. Experimental studies relating to microfracture in sandstone. Tectonophysics, 21: 203–247.

Hallbauer, D.K., Wagner, H. and Cook, N.G.W., 1973. Some observations concerning the microscopic and mechanical behaviour of quartzite specimens in stiff, triaxial compression tests. Int. J. Rock Mech. Min. Sci., 10: 713–726.

Handley, M.F., 1993. An investigation into the constitutive behaviour of brittle granular media by numerical experiment. Ph.D. Thesis, Univ. Minnesota.

Hoek, E. and Bieniawski, Z.T., 1965. Brittle fracture propagation in rock under compression. Int J. Fract. Mech. 1: 137–155.

Horii, H. and Nemat-Nasser, S., 1985. Compression induced microcrack growth in brittle solids: axial splitting and shear failure. J. Geophys. Res., 90: 3105–3125.

Kemeny, J.M. and Cook, N.G.W., 1987. Determination of rock fracture parameters from crack models for failure in compression. In: I.W. Farmer, J.J.K. Daimen, C.S. Desai, C.E. Glass and S.P. Neuman (Editors), Proc. 28th U.S. Symp. Rock Mech., Rotterdam, pp. 367–374.

Kemeny, J.M. and Cook, N.G.W., 1991. Micromechanics of deformation in rocks. In: S.P. Shah (Editor), Toughening Mechanisms in Quasi-brittle Materials. Kluwer, Dordrecht, pp. 155–188.

Kranz, R.L., 1983. Microcracks in rocks: a review. Tectonophysics, 100: 449–480.

Lajtai, E.Z., 1974. Brittle fracture in compression. Int. J. Fract., 10: 525–536.

Malan, D.F., Napier, J.A.L. and Watson, B.P., 1994. Propagation of fractures from an interface in a Brazilian test specimen. Int. J. Rock Mech. Min. Sci., 31: 581–596.

McClintock, F.A. and Walsh, J.B., 1962. Friction on Griffith

cracks in rocks under pressure. Proc. 4th U.S. Natl. Congr. Appl. Mech., New York, ASME, pp. 1015–1021.

Napier, J.A.L., 1990. Modelling of fracturing near deep level gold mine excavations using a displacement discontinuity approach. In: H.P. Rossmanith (Editor), Mechanics of Jointed and Faulted Rock. Balkema, Rotterdam, pp. 709–715.

Napier, J.A.L. and Hildyard, M.W., 1992. Simulation of fracture growth around openings in highly stressed brittle rock. J. S. Afr. Inst. Min. Metall., 92: 159–168.

Napier, J.A.L. and Ozbay, M.U., 1993. Application of the displacement discontinuity method to the modelling of crack growth around openings in layered media. In: A.G. Pasamehmetoglu (Editor), Proc. Assessment and Prevention of Failure Phenomena in Rock Engineering. Balkema, Rotterdam, pp. 947–956.

Nemat-Nasser, S. and Horii, H., 1982. Compression-induced nonplanar crack extension with application to splitting, exfoliation, and rockburst. J. Geophys. Res., 87: 6805–6821.

Olson, J.E. and Pollard, D.D., 1991. The initiation and growth of en echelon veins. J. Struct. Geol., 13: 595–608.

Olsson, W.A., 1974. Microfracturing and faulting in a limestone. Tectonophysics, 24: 277–285.

Petit, J. and Barquins, M., 1988. Can natural faults propagate under mode II conditions? Tectonics, 7: 1243–1256.

Reches, Z. and Lockner, D., 1994, Nucleation and growth of faults in brittle rocks. J. Geophys. Res., 99: 18,159–18,174.

Sammis, C.G. and Ashby, M.F., 1986. The failure of brittle porous solids under compressive stress states. Acta Metall., 34: 511–526.

Tapponier, P. and Brace, W.F., 1976. Development of stress-induced microcracks in Westerly granite. Int. J. Rock Mech. Min. Sci., 13: 103–112.

Thomas, A.L. and Pollard, D.D., 1993. The geometry of echelon fractures in rock: implications from laboratory and numerical experiments. J. Struct. Geol., 15: 323–334.

Wong, T.-f., 1982. Micromechanics of faulting in Westerly granite. Int. J. Rock Mech. Min. Sci., 19: 49–64.

Zheng, Z., 1989. Compressive stress-induced microcracks in rocks and applications to seismic anisotropy and borehole stability. Ph.D. Thesis, Univ. California, Berkeley, CA.